Brillouin scattering in glass-forming liquids: q-dependent linewidths and the generalized viscosity

H.Z. Cummins,[1] C. Dreyfus,[2] W. Götze,[3] G. Li,[1] and R.M. Pick[2]
[1] *City College, City University of New York, New York, New York 10031*
[2] *Departement de Recherches Physiques, Université Pierre et Marie Curie, 4 Place Jussieu, Paris 5, France*
[3] *Physik Department, Technische Universitat Munchen, D-85747 Garching, Germany and Max-Planck-Institut für Physik, Werner-Heisenberg-Institut, D-80805 München, Germany*
(Received 25 April 1994)

Recently, Gomperts, Variyar, and Kivelson [J. Chem. Phys. **98**, 31 (1993)] analyzed Brillouin linewidth data for triphenylphosphite and found a striking wave vector dependence which varied strongly with temperature. We present a simple explanation based on a Debye relaxation model from which results similar to theirs are obtained even though the longitudinal viscosity has no intrinsic wave vector dependence. We also explore the quantitative differences between their results and those obtained with the Debye model, and show that these differences can be explained by the two-step structural relaxation dynamics predicted by mode coupling theory and observed in recent neutron- and light-scattering experiments.

PACS number(s): 64.70.Pf, 78.35.+c, 83.50.Fc

Brillouin scattering (or ultrasonic) studies of liquids near and below the melting temperature T_m characteristically reveal a Brillouin linewidth $\Delta\omega$ (or ultrasonic attenuation) that increases with decreasing temperature, passes through a maximum, and then decreases again. The linewidth (or attenuation) maximum occurs when the average structural relaxation time τ, which increases monotonically with decreasing temperature, passes through $1/\omega_0$ where ω_0 is the Brillouin (or ultrasonic measurement) frequency.

This linewidth can be related to a generalized longitudinal viscosity $\eta_L(q,\omega)$ whose ω dependence, which is related to the structural relaxation dynamics, has been extensively investigated. However, there has been very little study of the q dependence of η_L, which can, in principle, probe the extent of spatial correlations that have often been discussed in connection with the liquid-glass transition. Furthermore, different q dependences of η_L may occur in fluids of neutral molecules or ionic fluids as discussed, e.g., by Giaquinta, Parrinello, and Tosi [1].

In a recent publication Gomperts, Variyar, and Kivelson (GVK) [2] analyzed the q dependence of Brillouin linewidths in the molecular glass-forming liquid triphenylphosphite determined from both conventional and time-resolved [3] Brillouin scattering experiments and found dramatic variation with temperature. They discussed several possible explanations for their results, including β relaxation and T_C phenomena of the mode coupling theory, but concluded that they did not have a theoretical interpretation of their data. In this article, we will first explore the origin of the qualitative features of their results and then consider their quantitative details.

The polarized (VV) light-scattering spectrum of a simple nonrelaxing fluid described by conventional linearized hydrodynamics can be written in a simple form if the very-low-frequency region containing the central thermal-diffusion mode is neglected:

$$I(\omega) = \frac{I_0}{\omega}\mathrm{Im}[\omega_0^2 - \omega^2 - i\omega\gamma^0]^{-1} \propto \frac{\gamma^0}{[\omega^2 - \omega_0^2]^2 + [\omega\gamma^0]^2}\ , \tag{1}$$

where $\omega_0 = C_0 q$ (C_0 is the adiabatic sound velocity). The damping constant γ^0 is given by [4]

$$\gamma^0 = \frac{q^2}{\rho}(\eta_B + \tfrac{4}{3}\eta_S) + q^2 D_T\left(\frac{C_P}{C_V} - 1\right). \tag{2a}$$

The second term in Eq. (2a), due to thermal diffusion, is usually small in nonmetallic liquids and will be ignored. The combination $(\eta_B + \frac{4}{3}\eta_S)$, where η_B is the bulk (or volume) viscosity and η_S the shear viscosity, is designated as the longitudinal viscosity η_L, so that

$$\gamma^0 \approx \frac{q^2}{\rho}\eta_L\ . \tag{2b}$$

From Eq. (1), if $\gamma^0 \ll \omega_0$, one finds that for ω close to ω_0,

$$I(\omega) \propto \left(\frac{1}{(\omega_0 - \omega)^2 + (\gamma^0/2)^2}\right). \tag{3}$$

The Brillouin components, centered at $\omega_B = \pm\omega_0 = \pm C_0 q$, are therefore Lorentzians with half width at half maximum

$$\Delta\omega = \gamma^0/2 = \frac{q^2}{2\rho}\eta_L\ . \tag{4a}$$

Equations (1)–(4a) follow from the Navier-Stokes equations, which describe liquids not exhibiting structural relaxation effects. (The absence of relaxation is indicated by the superscript on γ^0.) In order to describe liquids exhibiting structural relaxation, one can use Eq.

(4a) to define a generalized longitudinal viscosity $\eta_L^B = [\eta_L(q,\omega)]_{\omega=\omega_B(q)}$ in terms of the Brillouin linewidth $\Delta\omega$:

$$\eta_L^B = \frac{2\rho}{q^2}\Delta\omega \ . \tag{4b}$$

Fluids exhibiting structural relaxation are frequently described by introducing a relaxing memory function $m(t)$, with Laplace transform $m(\omega) = [i\int_0^\infty e^{izt}m(t)dt]_{z=\omega}$ into the hydrodynamic formalism. Equation (3) for $I(\omega)$ is then replaced by

$$I(\omega) \propto \frac{[\gamma + m''(\omega)]}{[\omega^2 - \{\omega_0^2 - \omega m'(\omega)\}]^2 + [\omega\{\gamma + m''(\omega)\}]^2} \ , \tag{5}$$

where γ is the frequency-independent damping, which is a generalization of γ^0 in Eq. (1) [i.e., γ contains all "fast" damping processes not explicitly represented by $m(\omega)$].

Momentum conservation requires that in the $q \to 0$ limit, both γ and $m(\omega)$ must be proportional to q^2. The resulting longitudinal viscosity $\eta_L = (\rho/q^2)[\gamma + m''(\omega = 0)]$ will exhibit intrinsic q dependence only if γ/q^2 or $m''(\omega = 0)/q^2$ depends on q.

The position of the Brillouin peaks ω_B is now determined by the roots of

$$[\omega^2 - \{\omega_0^2 - \omega m'(\omega)\}]^2 = 0 \ , \tag{6}$$

and the half width $\Delta\omega$ is given by

$$\Delta\omega = \frac{1}{2}[\gamma + m''(\omega_B)] \ . \tag{7}$$

Equation (5) is a generalization of Eq. (1), with all the unknown physics of structural relaxation hidden in $m(\omega)$, while Eqs. (6) and (7) are an approximation that is only valid if $m(\omega)$ is nearly constant over the frequency interval $\Delta\omega$. Equations (6) and (7) have been previously employed, e.g., in the interpretation of stimulated Brillouin scattering data [3].

The most elementary model for $m(t)$ is the Debye single-relaxation approximation $m_D(t) = \delta^2 e^{-t/\tau}$ for which [with the same Laplace transform convention used for Eq. (5)]

$$m'_D(\omega) = \frac{-\delta^2\omega\tau^2}{1+\omega^2\tau^2} \ , \tag{8a}$$

$$m''_D(\omega) = \frac{\delta^2\tau}{1+\omega^2\tau^2} \ . \tag{8b}$$

If one writes $\gamma = (q^2/\rho)\eta_\infty$ and $\delta^2 = (q^2/\rho)G_\infty$, Eqs. (8) then correspond to Maxwell's viscoelastic theory, where η_∞ and G_∞ denote the regular viscosity and the high-frequency longitudinal elastic modulus, respectively. In Maxwell's approach η_∞ and G_∞ are assumed not to show strong temperature dependence. The strong temperature dependence of $\eta_L = \eta_\infty + G_\infty\tau$ results from the temperature dependence of the Maxwell relaxation time τ.

The implications of Eqs. (8) for $I(\omega)$ were first analyzed by Mountain [5]. With this model for $m(\omega)$, Eq. (8a) predicts that the Brillouin components are centered at $\pm\omega_B$, where

$$\omega_B = \left(\omega_\infty^2 - \frac{\delta^2}{1+\omega_B^2\tau^2}\right)^{1/2} \ . \tag{9}$$

In Eq. (9), $\omega_\infty = (\omega_0^2 + \delta^2)^{1/2} = C_\infty q$ and C_∞ is the high-frequency adiabatic sound velocity. The Brillouin half width $\Delta\omega$ is given approximately by Eqs. (7) and (8) as

$$\Delta\omega \approx \frac{1}{2}\left(\gamma + \frac{\delta^2\tau}{1+(\omega_B\tau)^2}\right) \ . \tag{10}$$

Using the generalization of η_L suggested by Eqs. (4b) and (10), we find

$$\eta_L^B = \frac{\rho}{q^2}\left(\gamma + \frac{\delta^2\tau}{1+(\omega_B\tau)^2}\right) \ . \tag{11}$$

Note that η_L^B defined by Eq. (11) will exhibit q dependence even if γ/q^2, δ/q, τ, and, therefore, $[\eta_L(q,\omega)]_{\omega=\text{constant}}$ do not, because of the implicit q dependence of ω_B which is approximately proportional to q. However, for $\omega_B\tau << 1$, the generalized viscosity η_L^B reduces to the q-independent hydrodynamic limit discussed above.

Let us examine the implications of Eq. (10) for the quantities introduced by GVK in their linewidth analysis. To do this with realistic parameters, we start from the Brillouin scattering study of salol by Dreyfus *et al.* [6] (but neglecting the Cole-Davidson $\beta \neq 1$). We generated the $\Delta\omega(q,T)$ of Eq. (10) using a Vogel-Fulcher approximation for $\tau(T)$:

$$\log\tau(T) = -15.5 + 777/(T - 176) \tag{12a}$$

and temperature-independent values with "normal" q-dependence for the remaining parameters:

$$C_\infty = 2.1 \times 10^5 \text{ cm sec}^{-1} \ , \tag{12b}$$

$$\delta/q = 1.5 \times 10^5 \text{ sec}^{-1} \ , \tag{12c}$$

$$\gamma/q^2 = 0.01 \text{ sec}^{-1} \ . \tag{12d}$$

These parameters approximate the values found for salol ($T_m = 315$ K, $T_g \approx 218$ K) in Ref. [6].

Using these parameters, we calculated $\Delta\omega$ of Eq. (10) for T between 220 K and 320 K, for wave vectors q in the range

$$3.0 \leq \log_{10} q \leq 5.6 \ \ (\text{cm}^{-1}) \ ,$$

which is the same range studied by GVK. The resulting values of $\log_{10}(\Delta\omega)$ vs $\log_{10}(q)$ are shown in Fig. 1 for T= 220, 250, 290, and 330 K.

We next fit these data to the same fitting function utilized by GVK:

$$\Delta\omega = B(T)q^{\alpha(T)} . \tag{13}$$

The fits are also shown in Fig. 1 by the solid lines. In Fig. 2 we show the resulting values of $\log_{10}B$ and α. We find that $\alpha \approx 2.0$ at high and low temperatures, but exhibits a steep minimum at $T \sim 290$ K, near the temperature at which $\log B$ is a maximum. The results shown in Figs. 1 and 2 are qualitatively similar to those shown by GVK. It is surprising that the $\log(\Delta\omega)$ vs $\log(q)$ curves are so close to straight lines over a range of 2.5 decades in q which corresponds to the largest range covered by GVK. Like GVK we find oscillations around the straight line fit to our "data" for $T = 290$ K which is close to the temperature where Fig. 2(a) exhibits a maximum and Fig. 2(b) a minimum. Our results suggest that the indirect q dependence of $\Delta\omega$ due to the q dependence of ω_B makes it effectively impossible to infer the intrinsic q dependence of $\eta_L(q,\omega)$ from Brillouin linewidth data.

While the elementary Debye relaxation model explains the qualitative form of the GVK results, including the dip in α and the peak in B that occur between T_m amd T_g, quantitative differences remain. Comparing $\alpha(T)$ of Fig. 2 with Fig. 3 of GVK, two significant differences are observed. First, the minimum in $\alpha(T)$ found by GVK is ~ 0.9 while the minimum in Fig. 2 is more pronounced, ~ 0.4. Second, in Fig. 2, $\alpha(T)$ increases rapidly with decreasing T below the minimum, reaching $\alpha = 2$ at temperatures well above T_g. GVK, however, find that α increases slowly with decreasing T, reaching a maximum value of $\alpha \sim 1.3$ at T_g. Although these differences could be reduced by allowing the intrinsic damping constant γ in Eq. (10) to be temperature dependent, and replacing the Debye relaxation approximation by a stretched exponential (Kohlrausch) function, it is more instructive to explore the extent to which the quantitative form of $\alpha(T)$ found by GVK can be explained by invoking a more general description of $m(\omega)$.

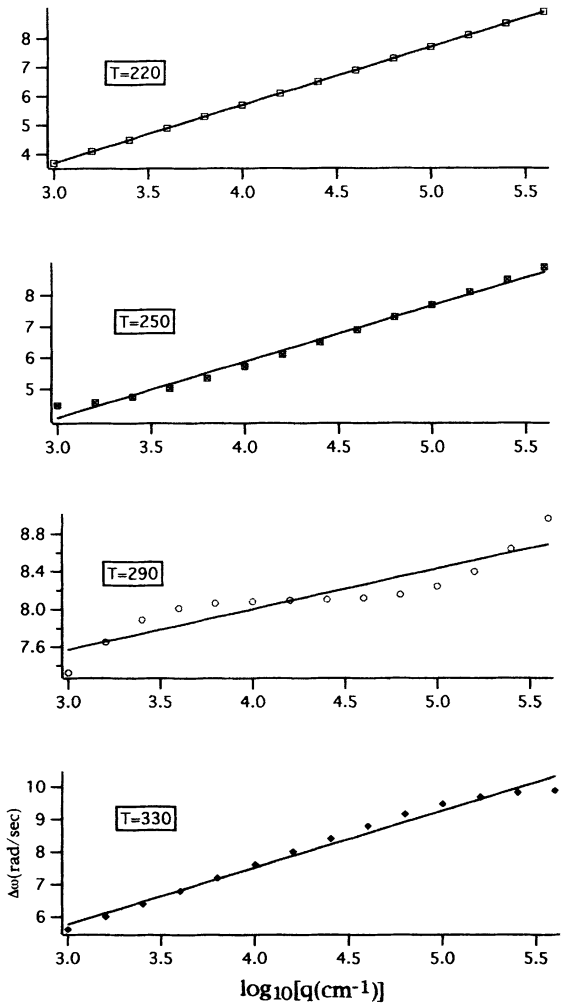

FIG. 1. $\log_{10}(\Delta\omega)$ vs $\log_{10}(q)$ found from Eq. (10) with the parameters of Eq. (12) (points) and linear fits (lines) for $T = 220$, 250, 290, and 330 K. Note that 330 K is above T_m while 220 K is $\sim T_g$.

In the remainder of this paper we will show how experimentally determined susceptibility spectra of supercooled liquids and theoretical predictions of the mode coupling theory can explain the GVK results. To this end we first reexpress $\Delta\omega$ of Eq. (7) in terms of a susceptibility spectrum $\chi''(\omega)$.

For the Debye model, $\chi_D(\omega) = \chi(0)/(1 - i\omega\tau)$ so that

$$\chi''_D(\omega) = \frac{\chi(0)\omega\tau}{1+\omega^2\tau^2} . \tag{14}$$

From Eqs. (8b) and (14),

$$m''_D(\omega) = \frac{\delta^2}{\omega\chi(0)}\chi''_D(\omega) . \tag{15a}$$

Note that $\delta^2 = (C_\infty^2 - C_0^2)q^2$, while $\omega_B = C_B q$. If we neglect the q dependence of C_B, then

$$m''_D(\omega) \propto \omega\chi''_D(\omega) , \tag{15b}$$

where the proportionality constant $= (C_\infty^2 - C_0^2)/C_B^2\chi(0)$.

Finally, we generalize Eq. (15b) to any $m''(\omega)$. Absorbing γ into χ'', Eq. (7) then becomes

$$\Delta\omega = D\omega_B\chi''(\omega_B), \tag{16}$$

where D is a q-independent constant. Equation (16) allows the q-dependent Brillouin linewidth $\Delta\omega$ to be predicted directly from the susceptibility function $\chi''(\omega)$. Note that the introduction of $\chi''(\omega)$ is merely a change of notation motivated by the common use of susceptibility spectra in the discussion of glassy relaxation.

Since $\omega = C_B q$, one finds for the exponent α in Eq. (13)

$$\frac{d[\log(\Delta\omega)]}{d[\log(q)]} = \frac{d[\log(\Delta\omega)]}{d[\log(\omega)]} = \alpha , \tag{17a}$$

while from Eq. (16),

$$\frac{d[\log(\Delta\omega)]}{d[\log(\omega)]} = 1 + \frac{d[\log(\chi''(\omega)]}{d[\log(\omega)]} . \tag{17b}$$

Therefore, we can write

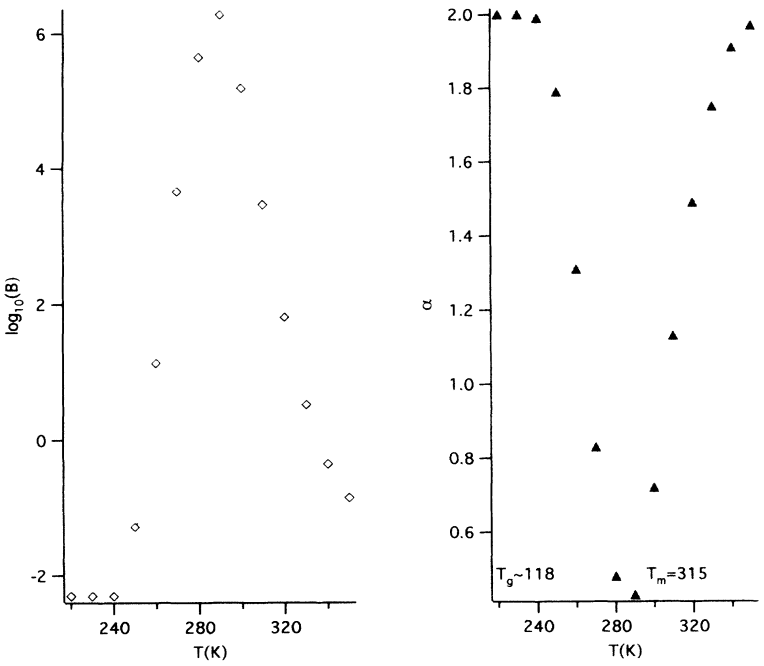

FIG. 2. Values of $\log_{10}B$ and α found from fits to Eq. (13). Note the steep minimum in α and maximum (incipient cusp) in $\log_{10}B$ near 280 K.

$$\alpha = 1 + S \tag{18}$$

where $S = \frac{d[\log\ \chi''(\omega)]}{d[\log\ (\omega)]}$ is the slope of the $\chi''(\omega)$ curve on a log-log plot.

Recent neutron- [7] and light-scattering [8] experiments have shown that in supercooled nonnetwork liquids $\chi''(\omega)$ exhibits a form in close agreement with predictions of the mode coupling theory (MCT) [9]. There is a low-frequency stretched α peak (a generalization of the Debye peak) which moves toward lower frequency with decreasing temperature, a high-frequency nearly T-independent microscopic (boson) peak, and between these two peaks the β-relaxation region centered on a minimum between the ω^{-b} high-frequency wing of the α peak and the ω^{a} critical decay spectrum leading to the boson peak.

In Fig. 3 we show a set of $\chi''(\omega)$ spectra for calcium potassium nitrate (CKN) found from depolarized light-scattering experiments [8,10]. These spectra have been extrapolated to frequencies below the experimental range (0.3 GHz–5 THz) by fitting the α peaks to Kohlrausch functions.

To illustrate the application of Eq. (18), we first show four theoretical susceptibility spectra $\chi''(\omega)$ in Fig. 4. They have been evaluated as solutions to the schematic F_{12} model of MCT (see Eq. (3.9a) in Ref. [9]). This model, which specifies mode coupling effects with only two coupling constants V_1 and V_2, was invented to demonstrate in a schematic manner some of the essential findings of the full MCT. The slope S is to be averaged over the frequency range (corresponding to the measured q range) indicated by the vertical dashed lines. In this figure, we have selected a smaller ω range than in Fig. 1 in order to demonstrate the evolution of slope S with temperature. The figure illustrates four specific situations that occur with decreasing temperature.

(1) At high temperatures, where the α peak is well above the measurement range, S is determined by the slope of the low-frequency wing of the α peak as $S = 1$ so that $\alpha = 2$.

(2) As T decreases, the α peak moves down through the measurement range, S decreases through $S = 0$ and reaches its minimum value of $S = -b$ when the measurement range coincides with the high-frequency (von Schweidler) wing of the α peak, so that $\alpha_{\min} = 1 - b$. Note that the maximum of B occurs when the Brillouin linewidth is largest, i.e., when the α peak moves through the center of the measurement range. This corresponds to $S = 0$ and therefore should occur at a temperature

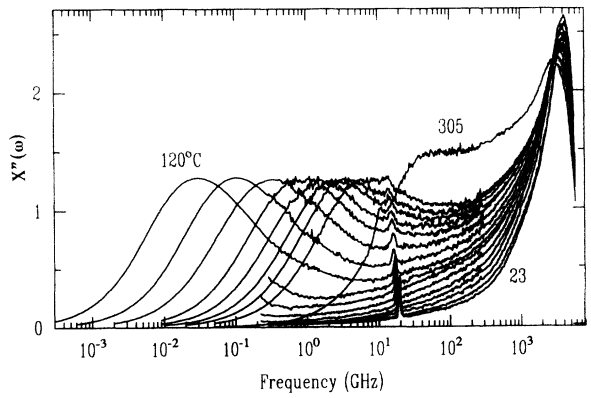

FIG. 3. $\chi''(\omega)$ spectra of CKN obtained from depolarized light-scattering experiments. The data were extended below 0.3 GHz by fitting the α peaks to Fourier-transformed Kohlrausch function (from Ref. [10]). The sharp lines near 20 GHz are residues of the longitudinal acoustic Brillouin components not removed by the polarizer.

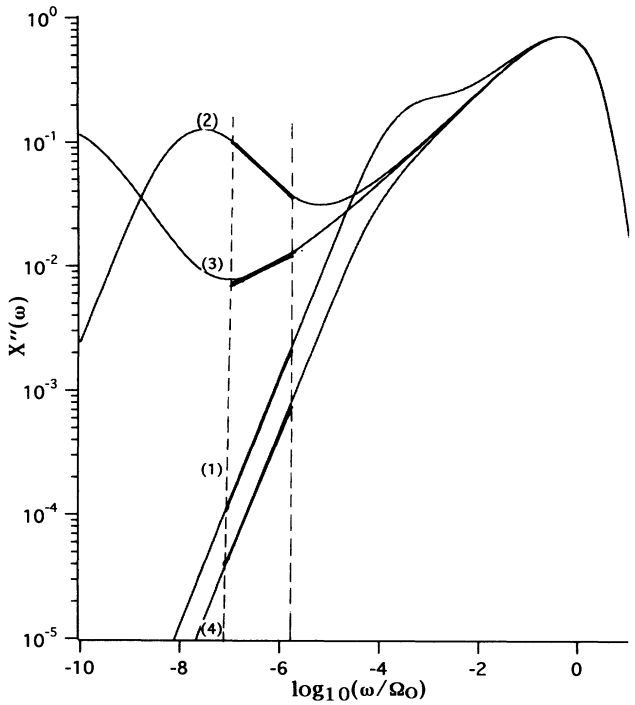

FIG. 4. $\chi''(\omega)$ computed with the schematic idealized F_{12} model of MCT with $\lambda = 0.7$, $a = 0.33$, $b = 0.64$, and $V_2 = 2.0$. For curves (1) – (3) ($T > T_C$), $V_1 = 0.828 - 0.4/2^n$ with $n = 2$ (curve 1), $n = 8$ (curve 2), $n = 12$ (curve 3). For curve (4) ($T < T_C$), $V_1 = 0.828 + 0.4/2^6$. [T decreases monotonically from (1) to (4).]

somewhat above that at which α reaches its minimum.

(3) With decreasing T the α peak moves completely out of the measurement range and so does the minimum of the β-relaxation region. S then increases through $S = 0$ up to a maximum $S = a$, the slope of the critical decay region, so that $\alpha = 1 + a$.

(4) When T decreases through T_C, the crossover temperature of MCT, the form of $\chi''(\omega)$ changes. The α peak and β minimum both disappear (in the idealized version of MCT considered here) and there appears a "knee" where the slope crosses over from $S = a$ above the knee to $S = 1$ below the knee. Since the knee moves to higher frequency with decreasing T, it should eventually move up through the experimental window and at sufficiently low temperatures α should increase from $\alpha = 1 + a$ to $\alpha = 2$. The temperature at which this increase will occur also depends on the range of q values included in the analysis.

We therefore expect that at high temperatures $\alpha = 2$; with decreasing T, α decreases monotonically to a minimum of $1 - b$. Then α increases again and reaches $1 + a$ for $T \sim T_C$, eventually increasing again to 2. The depth of the minimum and the value of the low-T maximum should thus be determined by the two critical exponents a and b. Whether this full range of $\alpha(T)$ will actually be observed, however, depends on the range of q values included in the experiment. Note that this discussion recovers the results of the Debye-model discussed earlier if one sets $a = b = 1$, assuming that γ has been included as shown in Eq. (5).

Another interesting result of this analysis can be seen by extending the ω range in Fig. 4 to more closely match the range in Fig. 1 and Ref. [2]. For intermediate temperatures [e.g., curve (2)], the slope will have significant variation with ω, leading to a departure from linearity as found by GVK. Also, since the *average* slope in this larger range will never reach $-b$, the minimum in $\alpha(T)$ will not reach the predicted lower bound of $1 - b$.

The preceeding discussion shows that the MCT for $m(\omega)$ implies results for $\alpha(T)$ which are closer to reality than the predictions of the simple Maxwell viscoelastic theory.

In Fig. 5 we have plotted $\alpha(T)$ found from an analysis of the CKN data of Fig. 3 following Eq. (18). The q range over which S was averaged for constructing Fig. 5 was again $3.0 \leq \log_{10} q \leq 5.6$, corresponding to $0.04 \leq \omega \leq 16$ GHz (with an average value for $C_B = 2.5 \times 10^5$ cm/sec). Our result for CKN in Fig. 5 is clearly closer to the experimental results of GVK than Fig. 2(b). Since we have shown in detail in Ref. [8] that the data in Fig. 3 fit the results of MCT, we conclude that this theory provides the essential explanation of the results reported by GVK.

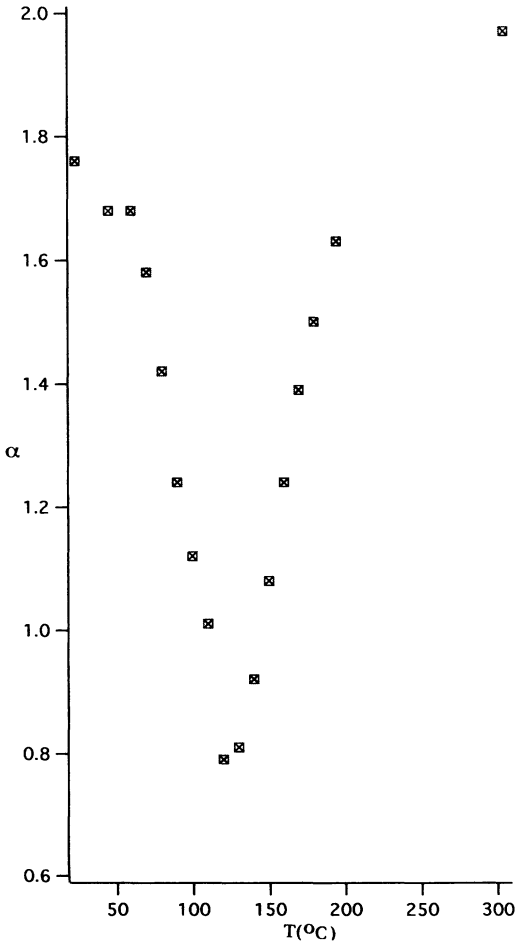

FIG. 5. $\alpha(T)$ vs T for CKN from fits of Eq. (18) to the CKN $\chi''(\omega)$ of Fig.3. The slope was averaged over the range 0.04 to 16 GHz, corresponding to the q range 10^3 to 4×10^5 cm^{-1}, taking $C_B = 2.5 \times 10^5$ cm/sec.

In conclusion, we have shown that the qualitative features found by GVK in their fits of Brillouin linewidth data to Eq. (13), a maximum in $B(T)$ and a minimum in $\alpha(T)$ somewhere between T_m and T_g, are simple consequences of structural relaxation that are predicted by any model, even the simple Debye model. The differences between the detailed predictions of the Debye model and the results of GVK indicate that the detailed relaxation dynamics affect the form of $\alpha(T)$ and $B(T)$. Although we consider it unlikely that Brillouin linewidth data can be interpreted to yield the actual form of the relaxation function, we have demonstrated that the $\chi''(\omega)$ found from other experimental and/or theoretical procedures can provide a consistent explanation of the GVK results.

We thank M. Fuchs for providing the program used to generate Fig. 4. This research was supported by NATO Collaborative Research Grant No. CRG-930730.

[1] P.V. Giaquinta, M. Parrinello, and M.P. Tosi, Physica **92A**, 185 (1978).
[2] S.N. Gomperts, J.E. Variyar, and D. Kivelson, J. Chem. Phys. **98**, 31 (1993).
[3] S.M. Silence, S.R. Goates, and K.A. Nelson, Chem. Phys. **149**, 233 (1990).
[4] B.J. Berne and R. Pecora, *Dynamic Light Scattering* (John Wiley & Sons, New York, 1976).
[5] R.D. Mountain, J. Res. Natl. Bur. Stand. **70A**, 207 (1966).
[6] C. Dreyfus, M.J. Lebon, H.Z. Cummins, J. Toulouse, B. Bonello, and R.M. Pick, Phys. Rev. Lett. **69**, 3666 (1992).
[7] F. Mezei, J. Non-Cryst. Solids **131-133**, 317 (1991).
[8] G. Li, W.M. Du, X.K. Chen, H.Z. Cummins, and N.J. Tao, Phys. Rev. A **45**, 3867 (1992).
[9] W. Götze and L. Sjögren, Rep. Prog. Phys. **55**, 241 (1992).
[10] G. Li, W.M. Du, J. Hernandez, and H.Z. Cummins, Phys. Rev. E **48**, 1192 (1993).